ELSEVIER

Polymer 42 (2001) 1481–1491

polymer

www.elsevier.nl/locate/polymer

Emulsion polymerization of styrene: double emulsion effect

Shi-Yow Lin[a,*], Chorng-Shyan Chern[a], Tien-Jung Hsu[a], Ching-Tien Hsu[a], I. Capek[b]

[a]*Department of Chemical Engineering, National Taiwan University of Science and Technology, 43 Keelung Road, Section 4, Taipei 106, Taiwan, R.O.C.*
[b]*Polymer Institute, Slovak Academy of Sciences, 842 36 Bratislava, Slovakia*

Received 24 March 2000; received in revised form 3 July 2000; accepted 11 July 2000

Abstract

Five independent sets of experiments have been performed in this work and some experimental evidence is presented to gain an insight into the reaction mechanisms of emulsion polymerization of styrene (St) stabilized by anionic emulsifier sodium dodecyl sulfate (SDS). Existence of water-in-oil-in-water (w/o/w) reverse micelles or double emulsion droplets is evidenced from the critical micelle concentration (cmc) measurement and the observation of w/o/w double emulsion experiment. Existence of monomer droplets at high monomer conversion and relatively low mass ratio of St/PSt in the swollen polystyrene (PSt) latex particles are demonstrated from the experiments of swelling of latex particles and the St emulsion polymerization. The increased uniformity and stability of the monomer emulsion is most likely due to the long pre-emulsification period and/or accumulation of PSt. This will then decrease the monomer droplet degradation, induce the formation of double monomer emulsion droplets and promote the apparent monomer-starved condition during polymerization. As a result, during polymerization the current polymerization system deviates from the conventional Smith–Ewart model, that is, the emulsion polymerization data show a distinct maximum R_p, the increase of N_p up to 20–50% conversion and a continuous increase in d_w in Intervals II and III. © 2000 Published by Elsevier Science Ltd.

Keywords: Emulsion polymerization; Double emulsion; Smith–Ewart model

1. Introduction

Emulsion polymerization involves the propagation of relatively water-insoluble monomers (e.g. styrene (St)) in submicron latex particles dispersed in an aqueous phase with the aid of surfactant (e.g. sodium dodecyl sulfate (SDS)). The polymerization process is generally divided into three distinct stages: nucleation of particle nuclei by capture of oligomeric radicals by the monomer-swollen micelles (Interval I), growth of latex particles by recruiting monomer and surfactant from the emulsified monomer droplets (Interval II), and depletion of residual monomer in the latex particles (Interval III) [1–4]. According to the Smith–Ewart theory (or the micellar nucleation model), the relationship $N_p \sim [S]^{0.6}[I]^{0.4}$ was established, in which N_p is the number of latex particles per unit volume of water and [S] and [I] represent the concentrations of surfactant and initiator, respectively. Reasonable agreement between the Smith–Ewart model and experimental data obtained from the St emulsion polymerization was reported [2–10]. On the contrary, deviation from the micellar nucleation model ($N_p \sim \rho_i^{0.27}$) was observed for the St emulsion polymerization initiated by sodium persulfate and stabilized by SDS [11]. The parameter $\rho_i = 2fk_d[I]$ is the production rate of initiator radicals in water and f and k_d are the initiator efficiency factor and the initiator decomposition rate constant, respectively. Both [S] and [I] were kept constant throughout that work and ρ_i was varied by changing the polymerization temperature ($T = 50$–$80°C$). Thus, the effect of ionic strength on the particle nucleation and colloidal stability of latex particles during polymerization can be eliminated. The recipe chosen for that study comprises 18.2 mM SDS, 1.4 mM $Na_2S_2O_8$ and 1.7 M St (based on total water), which is quite typical of conventional emulsion polymerization. The reactor system was equipped with four evenly spaced baffles and a 45° pitched six-bladed agitator. The average diameter of oil droplets in the reaction medium was found to decrease with time and then level off after the monomer emulsion was thoroughly mixed at 400 rpm for 1.5 h. Therefore, before the start of polymerization, the monomer emulsion was mixed at 400 rpm for 2 h to ensure that the emulsification is at steady state. To the best of our knowledge, such a long emulsification time has not been reported in the literature. The temperature and agitation speed were

* Corresponding author. Tel: +886-2-2737-6648; fax: +886-2-2737-6644.
E-mail address: ling@ch.ntust.edu.tw (S.-Y. Lin).

0032-3861/01/$ - see front matter © 2000 Published by Elsevier Science Ltd.
PII: S0032-3861(00)00526-7

kept constant within the range of ±0.5°C and at 400 rpm, respectively, throughout the reaction. The discrepancy was attributed to the following: (i) particle nuclei were continuously generated beyond Interval I; (ii) the range of Interval II became narrower when T increased from 50 to 80°C; (iii) desorption of free radicals out of the latex particles occurred when $T > 60$°C; and (iv) a significant population of tiny monomer droplets still remained in the reaction mixture beyond Interval II.

The objective of this study is to present more experimental evidence to explain why the St emulsion polymerizations at various temperatures (50–80°C) deviate from the Smith–Ewart model. First, the conductivity measurement was used to determine the critical micelle concentration (cmc) of the aqueous SDS solutions at different temperatures and the surface concentration of SDS at cmc (Γ_{cmc}) on the St macroemulsion droplet surface [12]. Values of cmc and Γ_{cmc} (surface concentration of SDS at monomer–water interface at cmc) provide valuable information about the concentration of micelles initially present in the reaction system, which is available for the subsequent particle nucleation, and the fraction of SDS molecules partitioned into the aqueous phase, oil–water interface and oil phase. A video-enhanced optical microscope was employed to measure the average diameter and particle size distribution of the St emulsion droplets and examine the morphologies of water-in-oil-in-water (w/o/w) double emulsion droplets observed in the course of polymerization and the particle swelling experiments. The w/o/w double emulsion consists of water droplets dispersed in larger St droplets; it is then dispersed in the continuous aqueous phase. The mechanism involved in the formation of w/o/w double emulsion droplets is proposed in this paper. Another major thrust for this work is to elucidate the effect of the w/o/w double emulsion and the increased stability of monomer droplets on the St emulsion polymerization kinetics. The swelling of dried polystyrene (PSt) latex particles by St is also used to study the transport of St from the monomer droplets to the reaction loci (i.e. PSt latex particles) during polymerization.

2. Experimental

Five sets of experiments were performed for the investigation of emulsion polymerization of St stabilized by anionic emulsifier SDS: (i) critical micelle concentration (cmc) measurement showing the existence of double w/o/w emulsion (i.e. w/o SDS reverse micelles/droplets inside the monomer droplets) in the St + SDS + water emulsion; (ii) preparation of double w/o/w emulsion and observation of the growth of monomer and double w/o/w droplets in the St + SDS + water emulsion; (iii) preparation of latex/emulsion mixtures illustrating the effect of PSt on the formation of double emulsion; (iv) swelling experiment evaluating the mass ratio of St/PSt in PSt latex particles; and (v) emulsion polymerization of St stabilized by SDS for the investigation of the reaction kinetics.

Materials. Emulsifier sodium dodecyl sulfate ($CH_3(CH_2)_{10}CH_2OSO_3Na$) was purchased from Fluka (SDS_1, >99% purity) and from Henkel (SDS_2, technical grade). Radical scavenger hydroquinone (HQ, $C_6H_4(OH)_2$, 99% purity) was from Nacalai Tesque, and initiator sodium persulfate (SPS, $Na_2S_2O_8$, 99% purity) was from Ridel-de Haen. These reagents were used as supplied. Commercially available styrene monomer (St, Taiwan Styrene Co) was distilled twice under reduced pressure before use. Water used throughout this work was purified via a Barnstead NANOpure water purification system with a specific conductance less than 0.057 μS/cm.

Measurement of cmc. The St + SDS_2 + water mixtures were emulsified at 25.0 ± 0.5°C in a baffled reactor with a 45° six-bladed downward impeller turbine. The reactor with a volume of 1.5 l was immersed in a water jacket, which was connected with a circulator in order to keep the emulsion at constant temperature. Anionic surfactant SDS_2 and 765 g water were first charged into this reactor. After SDS_2 was dissolved completely, 135 g St was added into the reactor [12]. The emulsion was then stirred at 400 rpm for 4 h. After emulsification, part of the emulsified product was transferred to a sample cell for the conductivity measurement. A video-enhanced optical microscope (Olympus, BH-2, Japan) was utilized to monitor and record the image of emulsion. The images were processed later for evaluating the average diameter and particle size distribution of the monomer droplets. Note that the St + SDS_2 + water emulsion at the time of conductivity measurement and image recording is kinematically stable and no coalescence of monomer droplets was observed during the monitoring and recording. The above process was repeated for different levels of surfactant with fixed amounts of water and St. From the slope break on the conductivity vs. surfactant concentration (κ–C) curve, cmc was then determined.

Two conductivity meters were employed for the conductivity measurement. The one for the aqueous SDS_1 (laboratory grade) solutions at 25.0 ± 0.2, 40, 50, 60, 70, and 80.0 ± 0.4°C was a conductivity meter with four electrodes (703, Knick, Germany). For St emulsions and aqueous SDS_2 solutions at 25.0 ± 0.2°C, a four-terminal cell with an impedance spectrometer was employed. This technique has been described in detail in previous studies [12,13]. Measurements were made in the frequency (ω) range between 0.1 Hz and 2 MHz. An electrical stimulus, $i(t) = I_m \sin(\omega t)$, was applied between counter electrode and working electrode and the resulting voltage $\nu(t) = V_m \sin(\omega t + \theta)$ between the reference electrodes was measured (Schlumberger SI 1286, England; controlled by a computer). Here θ is the phase difference between the voltage and the current. The impedance $Z(\omega)$ is defined as $\nu(t)/i(t)$ [14]. The values of solution resistance (R_s) of aqueous surfactant solutions and emulsions at different bulk concentrations were determined

from the impedance plane plot (the Nyquist diagram). The conductivity κ was then calculated (κ = cell constant/R_s).

St emulsion or aqueous SDS solution cmcs were deduced from the κ–C plots. The conductivity curves could be described by two straight lines. The break point in the κ–C plot indicates the cmc. The micelle ionization degree α was estimated from the ratio of the slope of the κ–C lines above and below cmc [15,16].

Preparation of w/o/w double emulsion. The ingredients of the recipe (765 g water, 135 g St, 18.2 mM SDS_1 (based on water), and 5 mM HQ (based on water)) were charged into the reactor (the one used in the cmc measurement) under the nitrogen atmosphere. The mixture was stirred at constant agitation speed (400 rpm) at 80°C for 72 h in the reactor. After remaining for 3 days at 80°C, the monomer emulsion was cooled down (without stirring) to room temperature and it separated into an upper oil-rich phase and a lower water-rich phase. During the stirring period, the emulsified solution was sampled and monitored using the video-enhanced optical microscope. The images of emulsion were also recorded. The images in tapes were processed later for evaluating the average diameter and particle size distribution of the double w/o/w emulsion and monomer (o/w) droplets.

Polymerization. The batch emulsion polymerization at 50–80°C with the recipe comprising 765 g water, 135 g St, 18.2 mM SDS_1 (based on water), and 1.4 mM SPS (based on water) was used to prepare the polymer latexes. The recipe chosen in this study is similar to those used in literature [7,17]. The size of the monomer droplets was examined by monitoring the solution sample using the video-enhanced microscope with 100× magnification. At 60°C, the average diameter of monomer droplets decreased with stirring time and then leveled off after 1.5 h. Therefore the St + water + SDS mixture was stirred for 2 h before the initiator was added to make sure that the polymerization had a very similar initial condition. This emulsification process ensured the transformation of the polydisperse monomer dispersion to a relatively monodisperse one.

The monomer conversion was determined by the gravimetric method. The average diameter and particle size distribution of polymer latex were determined by transmission electron microscopy (JEOL TEM-1200 EX II). During the reaction, the latex sample was taken and monitored by the video-enhanced optical microscope to obtain the population of the double emulsion (w/o/w) and monomer (o/w) droplets in the solution. Other conditions of the polymerization process and characterization techniques have been described in detail elsewhere [11,18]. Note that parts of the polymer latexes, prepared at 80°C, were dried at 50°C for 20 h and became the PSt powder used for preparing the monomer emulsion $\mathbf{B_2}$ (see the next section).

Latex/emulsion mixtures. Polymer latex (**A**) was first prepared using the above polymerization process at 80°C for 20 h to minimize the residual monomer. Monomer emulsion $\mathbf{B_1}$, with the recipe comprising 765 g water, 135 g St, 18.2 mM SDS_1 (based on water), and 5 mM HQ (based on water), was prepared at 25°C for 0.5 h in the reactor. Half of the cooled latex **A** (25°C) and half of the emulsion $\mathbf{B_1}$ were mixed together and formed a latex/emulsion mixture ($\mathbf{C_1}$) with an equivalent monomer conversion of 50%.

The other monomer emulsion $\mathbf{B_2}$ was prepared as follows. 4.5 g PSt powder was added into 67.5 g St monomer and mixed for 2 h using a magnetic stirrer. The monomer + polymer (St–PSt) solution was added into SDS solution (382.5 g water with 18.2 mM SDS_1 and 5 mM HQ, based on water) and then mixed for 0.5 h in the reactor. The second half of the cooled latex **A** was mixed with emulsion $\mathbf{B_2}$, and formed the second latex/emulsion mixture ($\mathbf{C_2}$) with an equivalent monomer conversion of 56.7%. Note that emulsion $\mathbf{B_2}$ and latex $\mathbf{C_2}$ have the same recipe as monomer emulsion $\mathbf{B_1}$ and latex $\mathbf{C_1}$, respectively, except the extra 4.5 g PSt premixed with St.

PSt latex swelling experiment. PSt latex was prepared using the above polymerization process, with 18.2 mM SDS_2 (based on water), at 80°C for 16 h. Anionic emulsifier SDS_2 was added to the solution, neglecting the initial SDS_2 in PSt latex solution, to make the SDS_2 concentration in aqueous phase equal to 6.7×10^{-6} mol/cm^3 (the cmc of SDS_2). Different amounts of St (0–4 g per g PSt) were then added into the PSt latexes (30 g, 15% PSt, at 25°C). The solution was kept at 25°C and stirred using a shaker at 125 rpm for 24 h to make sure that the solution reaches the equilibrium state. Scrap was found in each latex sample, but the weight is less than 1% of the total PSt latex. After the experiment, the solution was examined by the video-enhanced microscope to check the population of monomer droplets.

3. Results and discussion

Emulsion cmc. The conductivity data of aqueous SDS_2 solution and St + SDS_2 + water emulsion as a function of SDS concentration are plotted in Fig. 1. These data can be described perfectly by two straight lines and the break on the κ–C plot indicates the cmc of solution. The cmc of aqueous SDS_2 solution at 25°C is 6.7×10^{-6} mol/cm^3. The cmc of St + SDS_2 + water solutions at 25°C are 7.38, 7.44 and 7.72 (10^{-6} mol/cm^3) for three different runs, respectively, and an average of 7.5 ± 0.2 (10^{-6} mol/cm^3) is obtained. The data indicate that in this emulsion, 89.3% of added SDS molecules are in the continuous water phase and 10.7% of them either adsorb onto the St–water interface or go into the monomer droplet phase.

In a previous paper [12], the surface concentration of SDS at cmc at the St–water interface has been determined from the surface tension (γ) vs. surfactant concentration curve:

$$\Gamma_{\mathrm{cmc}} = -\frac{1}{(2-\alpha)\mathrm{R}T}\left(\frac{\partial\gamma}{\partial\ln C}\right) \quad (1)$$

where R is the gas constant, T is the absolute temperature, α is the micelle ionization degree, and Γ_{cmc} is the surface

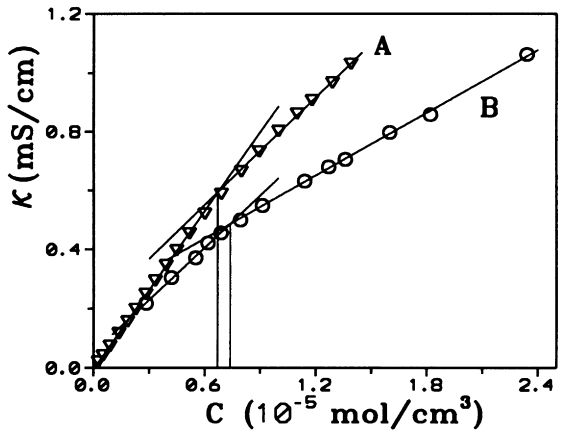

Fig. 1. Specific conductivity (κ in mS/cm) of: (A) aqueous SDS_2 solution (cmc = 6.7 mM at 25°C), and (B) St + SDS_2 + water macroemulsion (cmc = 7.38 mM at 25°C), plotted as a function of SDS_2 concentration.

concentration of SDS at cmc, evaluated from the slope of the γ–ln C plot near, but right below cmc (as shown in Fig. 9 of Ref. [12]). The value of α is estimated from the ratio of the slope of the κ–C lines above and below cmc. From the κ–C data, as shown in Fig. 1, a value of 0.62 ± 0.02 for α is obtained. The surface concentration of SDS at cmc is then calculated from Eq. (1) and Γ_{cmc} is equal to 3.54×10^{-10} mol/cm^2 at 25°C, i.e. the average area occupied by each SDS molecule is 46.9 Å^2. The surface concentration evaluated here is that for emulsion at cmc and SDS molecules adsorb at monomer–water interface as a monolayer.

The amount of SDS molecules adsorbed onto the oil–water interface was evaluated: $N_{o/w} = (\sum A_i) \times \Gamma_{cmc}$, where $\Gamma_{cmc} = 3.54 \times 10^{-10}$ mol/cm^2, A_i is the surface area of monomer droplet and $\sum A_i$ denote the total interfacial area of monomer droplets. The total monomer added in this emulsion is 135 g St per 765 g water. From the images of monomer droplets monitored using the video-enhanced microscope, the particle size distribution was obtained. The distribution of drop number per unit volume of emulsion (shown in Fig. 8 of Ref. [12] with a weight average droplet diameter of 8.9 ± 5.0 μm) was then obtained from the mass balance calculation. The above calculation indicates that 5.8% of the added SDS molecules adsorbed onto the monomer–water interface in emulsion at cmc. Besides the adsorbed SDS molecules and those in continuous water phase, 4.9% of the added SDS molecules in this emulsion is still missing. According to the following experiment, preparation of St + water + SDS emulsion stirred for 72 h, it is believed that this 4.9% of SDS molecules goes into the monomer phase and forms reverse micelles or tiny w/o/w droplets inside the St phase (i.e. the monomer droplets). More discussion follows.

The conductivity data of aqueous SDS_1 solution at different temperatures exhibit similar profiles as those shown in Fig. 1. The cmcs are 8.21, 8.48, 9.24, 9.98, 11.15, and 12.42 (10^{-6} mol/cm^3) for SDS_1 solutions at 25, 40, 50, 60, 70, and 80°C, respectively. These cmc data were used for the following experiments.

St + SDS_1 + water emulsion. Shown in Fig. 2 are images of the emulsion of St + SDS_1 + water (SDS_1 concentration = 1.47 × cmc) stirred at 400 rpm and 80°C for 72 h in the reactor. A w/o/w double emulsion was generated where both the internal and external phases are aqueous. The w/o/w droplets started to appear (big enough to be seen clearly using the microscope) after a few hours of stirring. More w/o/w droplets appeared with the stirring time. When the w/o/w emulsion formed, the internal and external aqueous phases were separated by the oily monomer phase. The two dispersed phases (w/o/w and o/w droplets) can be seen clearly in Fig. 2, especially at long stirring time. Thus, the one-step emulsification process with hydrophilic emulsifier SDS in the reaction mixture generates the unexpected w/o/w double emulsion.

Fig. 3 shows the dependence of the weight average radius of monomer droplets (R_w), the relative value of the total surface area of monomer droplets ($S_{o/w}/S_{o/w,t=2\ h}$), the polydispersity index of the droplet size distribution (PDI = R_w/R_n), and the number of monomer droplets (n_{oil}) per photograph. R_n is the number average radius of monomer droplets. R_w first increases to a maximum due to agglomeration and ripening of emulsion droplets. This is followed by a rapid decrease in R_w to a plateau because of the increased stability of emulsion droplets (i.e. formation of w/o/w double emulsion). This behavior is detailed in Fig. 3c, showing the variation of droplet fraction at different stirring times. The reverse is true for the $S_{o/w}$ data. It first decreases to a minimum, followed by an initial strong increase and then slight increase to a plateau, except the data point at 72 h. For the sample taken at 72 h, the fraction of monomer droplets with a radius of 3–10 μm decreases, whereas a larger fraction of 1–3 μm monomer droplets is observed (Fig. 3c). Therefore a larger value of $S_{o/w}$ is obtained at 72 h. Furthermore, the PDI data parallels roughly $S_{o/w}$. The number of monomer droplets (n_{oil}) per photograph (162×116 μm^2) remains nearly constant within the first 6 h, then increases monotonically with the stirring time.

The video-enhanced microscope can detect only those particles with radius (r) > 0.1 μm. It is reasonable to postulate that there are a lot of reverse SDS micelles and/or w/o/w emulsified water droplets within the monomer droplets. For those w/o/w droplets with $r > 0.1$ μm, the number average radius $(R_n)_{w/o/w}$ increases only slightly with the stirring time during the first 60 h, then more large water pools are observed and they show a rapid growth as shown in Fig. 4. The PDI data in Fig. 4 also indicate that the size of the w/o/w droplets is quite uniform at the initial 60 h of stirring. The w/o/w double emulsion is quite sensitive to temperature since the w/o/w droplets become smaller when the emulsion is cooled down from 80 to 25°C (as shown by the closed marks in Fig. 4).

Considering the data presented in the above section, 5.8% of SDS molecules adsorb onto the o/w interface in emulsion

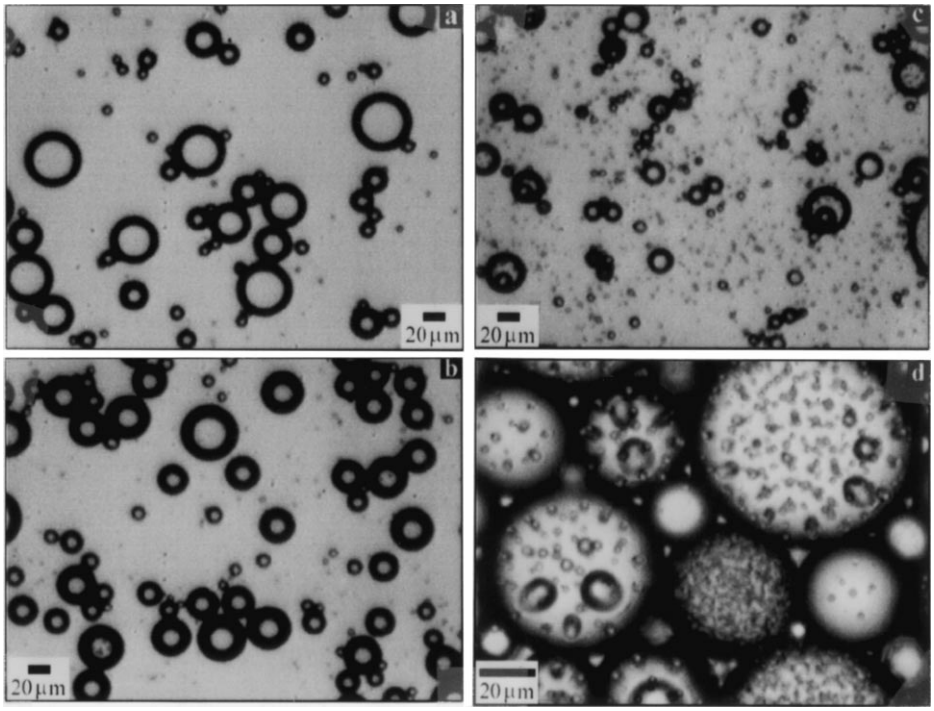

Fig. 2. Variation of monomer droplet size, structure and number with swelling time. Stirring rate = 400 rpm, temperature = 80°C. Swelling time: (a) 2, (b) 8, and (c) 72 h; magnification = 40×. Part (d) is the oil (upper) phase of emulsion, after 72 h stirring at 80°C and then cooling down to 25°C. For recipe, see experimental part.

at cmc and 4.9% of SDS molecules was missing. The experiment in this section demonstrates that there exist reverse SDS micelles and/or w/o/w emulsified water pools inside the monomer droplets. It is the SDS molecules adsorbed on these reverse micelles and/or w/o/w double emulsion droplets that are responsible for the missing SDS species. The w/o/w droplets also grow with the stirring time, from 0.9 to 1.5 μm in R_n or from 1.0 to 4.2 μm in R_w for those w/o/w droplets larger than 0.1 μm.

Latex/emulsion mixtures. Polymer latex **A** has an average diameter of 58 nm (D_w) and a narrow size distribution (PDI = 1.07) [11]. No w/o/w droplets were observed by the microscope (i.e. $r < 0.1$ μm) for monomer emulsion $\mathbf{B_1}$ (which had been stirred only for 0.5 h), whereas for $\mathbf{B_2}$, many w/o/w emulsion droplets inside the monomer droplets were observed, as illustrated in Fig. 5.

The PSt dissolved in the monomer droplets just acts as a hydrophobic reagent to retard the molecular diffusion of the monomer from small monomer droplets to large droplets (termed the Ostwald ripening effect) [19–21]. This osmotic pressure effect will increase the stability of monomer droplets. This will then promote the formation of the w/o/w emulsion droplets [22]. Latex/emulsion mixtures of $\mathbf{C_1}$ and $\mathbf{C_2}$ at different stirring times are monitored by the video-enhanced microscope. Two representative images of the mixtures of $\mathbf{C_1}$ and $\mathbf{C_2}$ at stirring time = 2 h are shown in Fig. 6. Images show that the $\mathbf{C_1}$ and $\mathbf{C_2}$ samples have nearly the same o/w droplets.

Figs. 5 and 6b ($X = 6.7$ and 56.7%, respectively) indicate that PSt latex particles absorb St and form the swollen PSt particles, whose diameter is smaller than 0.2 μm. The mass ratio of St to PSt in the swollen PSt particles is less than 1. This is because the mass ratio of St to PSt is 1/1 in $\mathbf{C_1}$ (with an equivalent monomer conversion of 50%) and there still exist many monomer droplets in the $\mathbf{C_1}$ sample. The mass ratio of St to PSt in the swollen PSt particles was found to be around 0.15/1 from the following experiments. The mechanism involved in the formation of w/o/w double emulsion stabilized by SDS is not clear at this time and further research is required.

Swollen PSt latex particles. No monomer droplets (i.e. $r < 0.1$ μm) were detected using the microscope when less than 0.143 g St (per g PSt) was added into the PSt latex with the SDS concentration being around cmc. When more than 0.151 g St (per g PSt) was added, there existed monomer droplets (i.e. $r > 0.1$ μm) in the latex sample. More and larger monomer droplets were found when more St was added into the latex. Two representative images (0.215 and 0.848 g St per g PSt) obtained from the optical microscope are shown in Fig. 7. The number average radius of monomer droplets (R_n) and the number of monomer droplets per photograph (n_{oil}, 62×29 μm^2) are also shown in Fig. 7. Data obtained from the particle swelling experiments indicate that there exist monomer droplets in the latex sample when the mass ratio of St/PSt ($= R_{m/p}$) in the swollen PSt latex particles is larger than 0.15/1. That is, monomer droplets will not disappear until the $R_{m/p}$ value is less than 0.15/1. It is generally accepted that St molecules

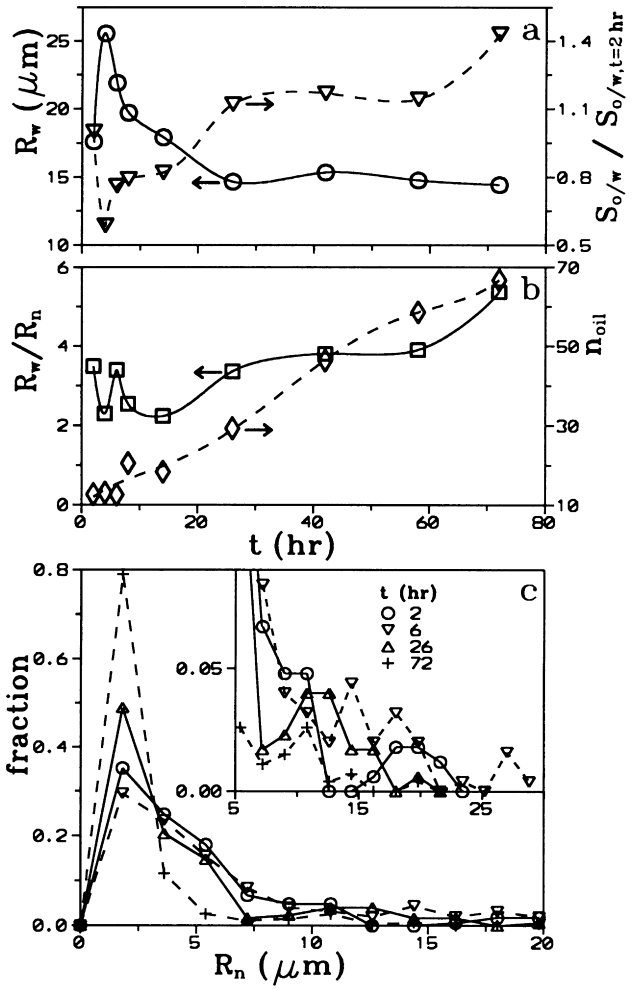

Fig. 3. Variation of: (a) monomer droplet radius (R_w) and droplet surface area (S_{area}), (b) droplet size distribution (R_w/R_n) and the number of droplets per photograph ($417 \times 289\ \mu m^2$) with stirring time, and (c) monomer droplet fraction with number average droplet size (R_n) at different stirring times. Stirring rate = 400 rpm, temperature = 80°C.

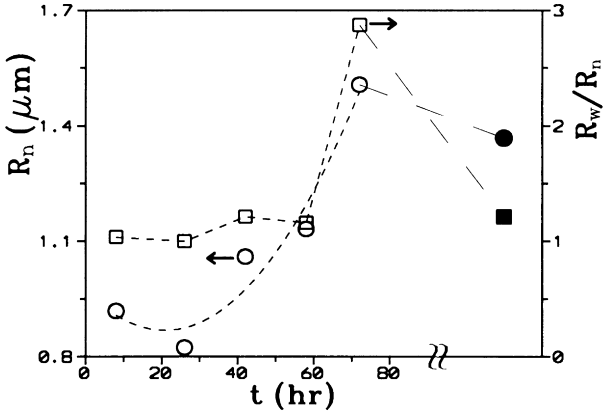

Fig. 4. Variation of w/o/w droplet radius $(R_n)_{w/o/w}$ and droplet size distribution $(R_w/R_n)_{w/o/w}$ with stirring time. Stirring rate = 400 rpm, temperature = 80°C. The solid marks represent the data of >72 h and at 25°C.

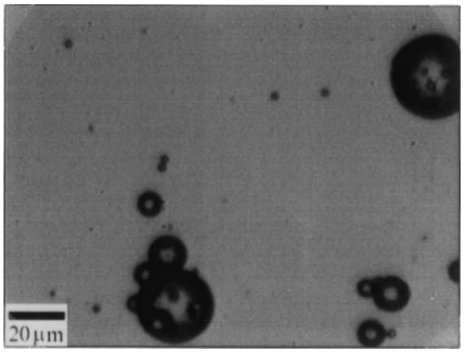

Fig. 5. Double emulsion droplet structure (100×) of monomer emulsion $\mathbf{B_2}$. Stirring rate = 400 rpm, T = 80°C.

prefer to diffuse from the monomer droplets to the monomer-starved PSt particles until an $R_{m/p}$ value of 1.42/1–1.55/1 is achieved [3,4,17,23,24]. The contradictory $R_{m/p}$ data between the present work and the literature implies that resistance to diffusion of St molecules from monomer droplets to PSt latex particles unsaturated with monomer builds up rapidly when SDS and/or PSt are present inside the monomer droplets.

Polymerization kinetics. Fig. 8 shows the variation of the polymerization rate (R_p), weight average diameter of dried latex particles (d_w), and number of latex particles per liter water (N_p) with monomer conversion (X) for emulsion polymerization of St at 50, 60, 70 and 80°C. Fig. 8a, c and d has been reported in Ref. [11]. In classical emulsion

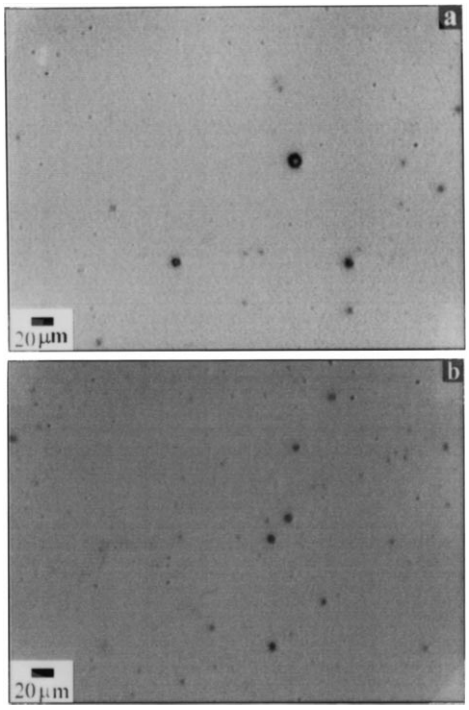

Fig. 6. Images of monomer droplets (40×) for mixtures: (a) $\mathbf{C_1}$, and (b) $\mathbf{C_2}$ at stirring time = 2 h. Stirring rate = 400 rpm, T = 80°C. For recipe, see experimental part.

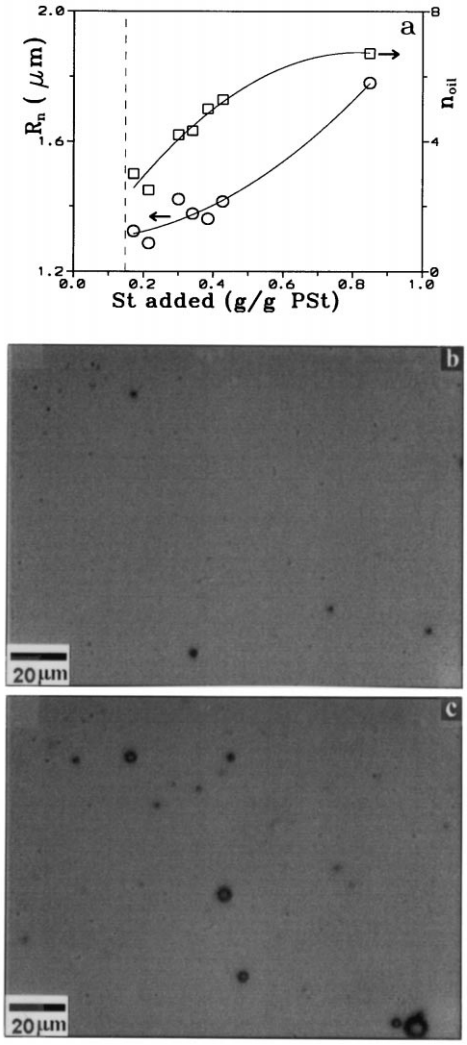

Fig. 7. Variation of number average radius of monomer droplets and the number of monomer droplets per photograph (a) and representative images of monomer droplets for the solution of swelling experiment with St/PSt mass ratio = 0.215 (b) and 0.848 (c) at 25°C. For recipe see experimental part.

polymerization of hydrophobic monomers (e.g. St), both N_p and R_p increase with increasing X during Interval I, which ends around 5–10% conversion [25,26]. In Interval II (X = 10–50%), R_p remains relatively constant and the latex particle size increases as the polymerization proceeds. Subsequently, the particle size remains relatively constant toward the end of polymerization. In the present study, the R_p–X curve in Fig. 8a and b, however, shows one distinct maximum at ca. 20–40% conversion. It is also interesting to note that the polymerization temperature does not show a significant effect on the normalized polymerization rate vs. conversion profile (Fig. 8b). The parameter $R_{p,max}$ appearing in the ordinate of Fig. 8b is the maximum polymerization rate.

During the early stage of polymerization, the rapidly increased R_p with X is attributed to the high generation rate of initiator radicals in water (ρ_i) and intensive particle nucleation. In addition, formation of free radicals via the thermally induced polymerization further increases R_p for the polymerization carried out at higher T [27]. N_p increases up to 20–50% conversion (beyond Interval I) and d_w increases throughout the reaction (Fig. 8c and d). Thus, the higher the polymerization temperature, the more pronounced the continuous particle nucleation. The cmc of the aqueous SDS solution increases with increasing T. Neglecting the influence of the monomer, the cmc data suggest that the initial concentration of micelles available for particle nucleation decreases with increasing T. On the other hand, ρ_i increases with increasing T and, moreover, desorption of free radicals out of latex particles becomes more important when T increases from 50 to 80°C [11]. The concentration of free radicals in the aqueous phase then increases significantly with increasing T. As a result, the higher the reaction temperature, the larger the probability that the micelles capture oligomeric radicals from the aqueous phase to induce micellar nucleation.

Homogeneous nucleation [28–30] may also occur because the particle nuclei born in the aqueous phase can be stabilized by those SDS molecules dissolved in water, those released from the disbanded micelles and those desorbed out of the latex particle surfaces and monomer droplets. As mentioned above, about 5.8% of the initially added SDS molecules is adsorbed on the monomer droplet surfaces in emulsion at cmc and 4.9% of the SDS molecules is adsorbed at the interface of the w/o reverse droplets dispersed inside the monomer droplets. The (double) monomer emulsion droplets, abundant in SDS, can supply both the growing latex particles and particle nuclei generated in the aqueous phase with surfactant. Fig. 9 shows two representative images for the reaction mixture taken at early conversion (X = 7.1 and 18.6%) for the St polymerization at 60°C. The w/o/w droplets can be clearly observed. Similar results are also observed for the polymerization system carried out at other temperatures. In addition, the increased fraction of emulsifier in water with temperature promotes the interaction of radicals with the emulsifier and, thereby, enforces the contribution of homogeneous nucleation to the relatively long particle-formation process. The increased water solubility of monomer and concentration of the initiator radicals with temperature may also increase the concentration of the surface active St oligomer in the aqueous phase, thereby leading to the increased importance of homogeneous nucleation. Recently, Chern and Lin [31] used a water-insoluble dye as the probe to demonstrate that a significant population of PSt latex particles originates from homogeneous nucleation when the SDS concentration is above the cmc.

Immediately after the maximum is reached, R_p starts to decrease toward the end of polymerization, whereas d_w continues to increase with increasing X (Fig. 8c). The preservation of monomer droplets accompanied with the restricted diffusion of monomer from the monomer droplets to the monomer-starved latex particles promotes

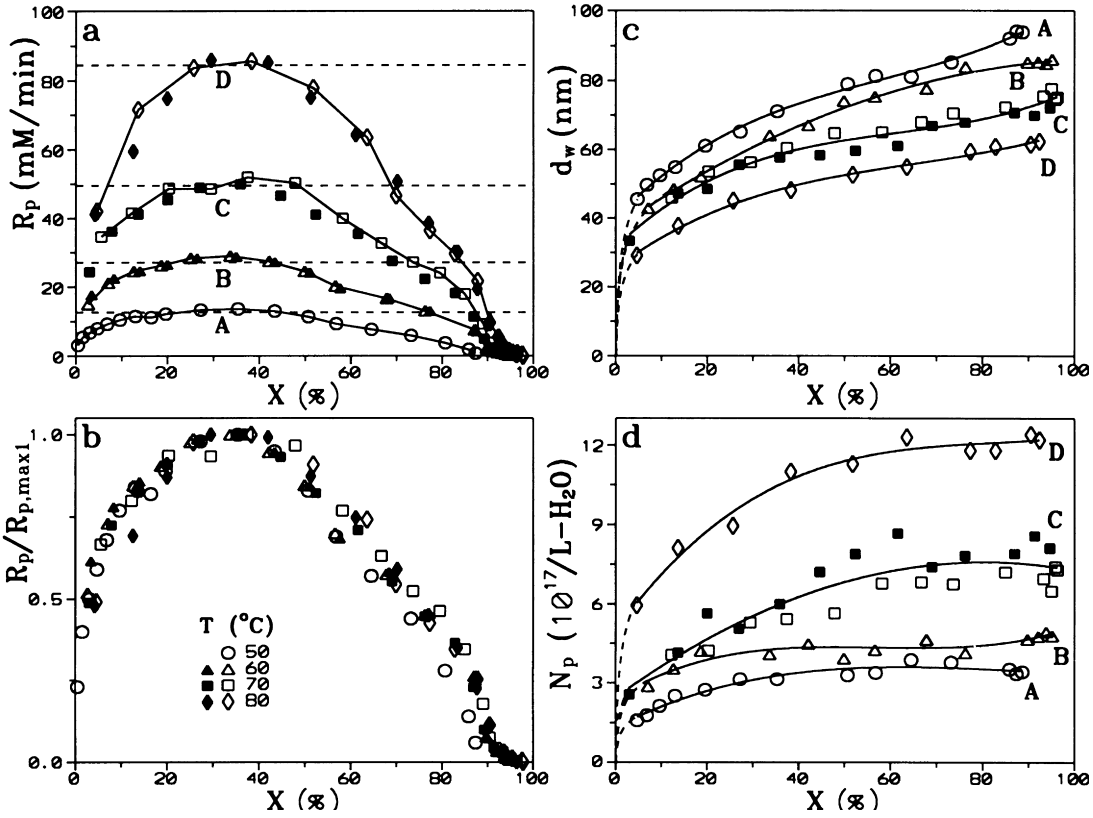

Fig. 8. Variation of polymerization rate (R_p) and ratio of $R_p/R_{p,max}$ with monomer conversion (a, b), particle diameter (d_w) with conversion (c), and number of particles (N_p) with conversion in emulsion polymerization of St at different temperatures. For recipe see experimental part.

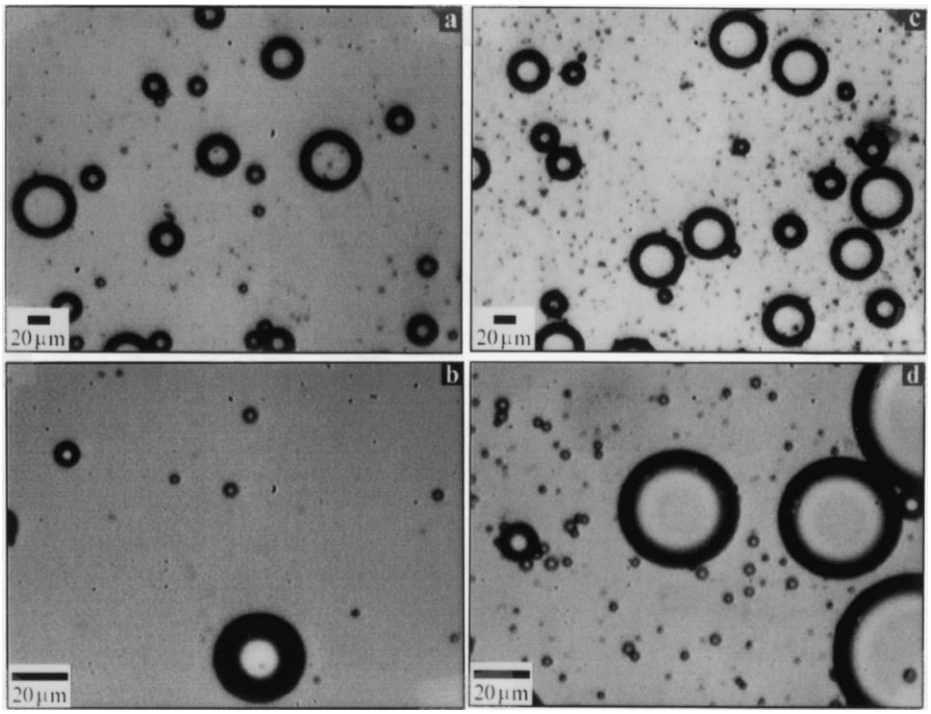

Fig. 9. Variation of monomer and w/o/w emulsion droplets with monomer conversion, 7.1% (c, d), and 18.6% (a, b), in emulsion polymerization of St at 60°C. Magnification 40× (a, c) and 100× (b, d).

the continuous formation of surface active oligomer. The surface active oligomer increases the stability of latex particles and contributes to the formation of latex particles up to 20–50% conversion (Fig. 8a and d). The rapidly increased total particle surface area and greatly reduced monomer transfer beyond ca. 40–50% conversion then depress the participation of these surface active species in the particle-formation process, i.e. oligomeric radicals are absorbed by the latex particles before reaching the critical degree of polymerization for precipitation. Beyond Interval II, these monomer droplets supply the latex particles with monomer and, therefore, d_w continues to increase gradually with increasing X.

It is postulated that accumulation of SDS and PSt at the internal w/o interface increases the stability of the w/o/w double emulsion droplets and, thereby, retards the diffusion of monomer to the reaction loci (growing latex particles). This is further supported by the mass balance that about 4.9% of the SDS molecules is adsorbed at the interface of the w/o reverse droplets dispersed inside the monomer droplets (see the above discussion). The presence of hydrophobe, e.g. PSt, in this work in the monomer phase increases the stability of double emulsion droplets [32]. This may be the reason why a significant population of monomer droplets can survive up to 95% conversion in this study, which is much higher than that reported in the literature (ca. $X = 40$ to 60%) [1,7,17,23,24,32,33]. The PSt containing droplets may become smaller during polymerization, but they are unlikely to disappear completely via diffusion of monomer to the growing latex particles [20,21,33]. The gradually shrinking droplets ultimately become so small that they can be detected only up to ca. 95% conversion. This behavior probably relates to the very low $R_{m/p}$ data obtained from the swelling experiments (see the above section of swollen PSt latex particles). In addition, R_n decreases with increasing X and the most significant reduction in the droplet size occurs in the low conversion range (Fig. 10). In the low concentration range, the increase of both d_w and N_p is also the most pronounced. Under the circumstances, the aqueous phase is saturated by monomer (i.e. diffusion of monomer from the monomer droplets to the reaction loci is not restricted) and both the particle nucleation and growth processes proceed without problem. The rapid increase of d_w with X may also result from the particle agglomeration when homogeneous nucleation is operative. In this study, the monomer droplets will not disappear (i.e. R_n is still larger than 0.1 μm) until $X = 95$ to 98%. Fig. 10 shows the variation of R_n and n_{oil} (number of monomer droplets per photograph, $417 \times 289\ \mu m^2$) as a function of X for the polymerizations at 60, 70, and 80°C. The presence of monomer droplets at high conversion observed in the current study deviates from the Smith–Ewart theory. Note that the n_{oil} at 70°C for $X = 10$–70% is small. The reason is not clear at present, but it is most likely because of the large sampling error on this particular run.

Although monomer droplets are present in the reaction system beyond Interval II, the monomer concentration in the latex particles continues to decrease with increasing X. As a result, the polymerization proceeds under the apparent monomer-starved condition (the monomer droplets are still present) and R_p decreases toward the end of the reaction. Fig. 8c shows that latex particles continue to grow throughout the polymerization. This is most likely due to the presence of rather stable monomer droplets (simple or double emulsion droplets) dispersed in the reaction medium, which partially provides the growing latex particles with monomer. The simple monomer droplets are stabilized by accumulation of PSt in the droplets. The continuous penetration and accumulation of SDS and PSt at the internal w/o interface and the monomer phase result in a close-packed structure therein and improve the stability of the w/o/w emulsion. Under the circumstances, diffusional degradation of monomer droplets is greatly retarded [20,21]. Furthermore, the suppressed monomer diffusion to the growing latex particles is responsible for formation of latex particles with relatively narrow particle size distribution (PDI = 1.04 (50°C)–1.14 (80°C)). It should be noted that, at the level of shear force used to prepare the monomer emulsion, the emulsified monomer droplets are not small enough to induce the predominant nucleation and polymerization in the droplets (termed the miniemulsion polymerization), as shown by the optical microscopy data. Thus, the micellar and/or homogeneous nucleation mechanisms play an important role in the particle formation and growth processes.

Finally, St can polymerize in the absence of initiator when T is above 60°C. Several emulsification experiments at various temperatures were then carried out to verify whether such thermal polymerization occurs after the monomer emulsion is thoroughly mixed at 400 rpm for

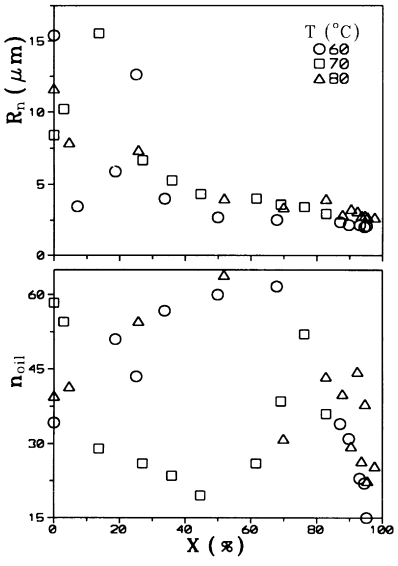

Fig. 10. Variation of monomer droplet radius (R_n) and droplet number per picture (n_{oil}) with monomer conversion in emulsion polymerization of St at different temperatures.

2 h. The monomer conversions achieved are 0.02 (50°C), 0.10 and 0.93% (70°C). The true levels of conversion achieved should be much larger because isolation of a small amount of polymer from the emulsified system by the precipitation method results in the loss of a large fraction of polymer and especially polymer of low molecular weight. Although the effect of thermal polymerization on the initial X vs. t profiles is not significant [11], the increased uniformity and stability of monomer droplets may also have an impact on the reaction kinetics at medium and high conversion. The increased uniformity of the initial emulsion by a long pre-emulsification period is reported to retard the Ostwald ripening [34]. The monodisperse monomer emulsion droplets show much higher resistance against flocculation as compared to the polydisperse counterpart of the same recipe [35]. The presence of ca. 0.5 wt% predissolved PSt improves the stability of St miniemulsion droplets signicantly [36]. Thus, a similar behavior is expected for the St emulsion polymerization with the accumulation of PSt in the monomer phase during emulsification period (2 h at 60°C) and polymerization (2–4 h) [27]. The initial formation of St oligomer is not ruled out owing to the presence of a small amount of impurities and oxygen, which react with oligomeric radicals. Furthermore, the polymer produced in the monomer phase enhances the stability of the o/w monomer droplets and, thereby, decreases the diffusion of monomer from the monomer droplets to the growing latex particles in the subsequent emulsion polymerization. As a result, a significant population of monomer droplets still can be observed beyond Interval II, which is inconsistent with the Smith–Ewart theory.

In addition to the reaction mechanisms proposed by Chern et al. (see Section 1) [11], this work has provided more experimental evidence to explain why the St emulsion polymerizations at various temperatures deviate from the conventional Smith–Ewart theory. This work clearly illustrate the presence of w/o/w emulsion droplets inside the monomer droplets. Resistance against the diffusion of monomer from the o/w monomer droplets to the growing latex particles results from the osmotic pressure effect provided by the accumulation of PSt inside these droplets. This will lead to the reduced monomer concentration in the reaction loci and then slow down the polymerization. The thermal polymerization in the monomer droplets does not contribute significantly to increase the total amount of polymer produced, but the accumulation of PSt in these droplets is partially responsible for the enhanced droplet stability. The polymerization mechanism involved, however, is still not clear at this time and further research is required.

4. Conclusions

The St emulsion polymerization mechanism was investigated via five independent sets of experiments. The video-enhanced optical microscopy provides evidence for the existence of the w/o/w emulsion droplets. Measurement of cmc of St + SDS + water emulsion along with a mass balance indicate the accumulation of emulsifier within the monomer phase. Furthermore, the accumulation of polystyrene (PSt) in the reaction system enhances the stability of monomer droplets as well as the formation of w/o/w double emulsion. The swelling experiment and examination of latex samples during emulsion polymerization demonstrate the existence of monomer droplets at high monomer conversion and the relatively low mass ratio of St/PSt in the swollen PSt latex particles (Interval II). The latter is the result of the polymerization proceeding under the monomer-starved condition. The increased uniformity and stability of the initial monomer emulsion as a result of the relatively long pre-emulsification period at 50–80°C and accumulation of PSt are connected with the depressed monomer droplet degradation and shift of the monomer-starved condition to low conversion. Under the circumstances, the emulsion polymerization data show a distinct maximal R_p, and a continuous increase in d_w with conversion during Intervals II and III and the increase of N_p up to 20–50% conversion. Based on the experimental data presented in this work, the root cause for the peculiar behavior observed in the St emulsion polymerization is the relative stable and uniform monomer emulsion prepared by the pre-emulsification method used. What has been done in this work is to present some interesting experimental evidence on the St emulsion polymerization, and attempt to explain why the current system deviates significantly from the micelle nucleation model.

Acknowledgements

The financial support from National Science Council, Taiwan, is gratefully acknowledged (Grant NSC 88-2214-E-011-015).

References

[1] Harkins WD. J Am Chem Soc 1947;69:1428.
[2] Smith WV, Ewart RW. J Chem Phys 1948;16:592.
[3] Smith WV. J Am Chem Soc 1948;70:3695.
[4] Smith WV. J Am Chem Soc 1949;71:4077.
[5] Barthalome E, Gerrens H, Herbeck R, Weitz HM. Z Elektrochem 1956;60:334.
[6] Manyasek Z, Rezabek A. J Polym Sci 1962;56:47.
[7] Omi S, Sato H, Kubota H. J Chem Engng Jpn 1969;2:55.
[8] Chatterjee SP, Banerjee M, Konar RS. J Polym Sci Polym Chem Ed 1978;16:1517.
[9] Chern CS, Lin SY, Chen LJ, Wu SC. Polymer 1997;38:1977.
[10] Chern CS, Lin SY, Chang SC, Lin JY, Lin YF. Polymer 1998;39:2281.
[11] Chern CS, Lin SY, Hsu TJ. Polym J 1999;31:516.
[12] Chang HC, Lin YY, Chern CS, Lin SY. Langmuir 1998;14:6632.
[13] Chang HC, Hwang BJ, Lin YY, Chen LJ, Lin SY. Rev Sci Instrum 1998;69:2514.
[14] Macdonald JR. Impedance spectroscopy. New York, 1987 (chap. 4).
[15] Zana R. J Colloid Interface Sci 1980;78:330.
[16] Lianos P, Lang J. J Colloid Interface Sci 1983;96:222.

[17] Harada M, Nomura M, Kojima H, Eguchi W, Nagata S. J Appl Polym Sci 1972;16:811.
[18] Lin SY, Capek I, Hsu TJ, Chern CS. J Polym Sci Polym Chem Ed 1999;37:4422.
[19] Kabalnov AS, Shchukin ED. Adv Colloid Interface Sci 1992;38:69.
[20] Reimers J, Schork FJ. J Appl Polym Sci 1996;59:1833.
[21] Reimers J, Schork FJ. J Appl Polym Sci 1996;60:251.
[22] Kim JW, Joe YG, Smith KD. Colloid Polym Sci 1999;277:252.
[23] Vanzo E. PhD thesis. State College of Forestry, Syracuse University, Syracuse, NY, 1962.
[24] Chiu WY, Shih CC. J Appl Polym Sci 1986;31:2117.
[25] Blackley DC. Emulsion polymerization. London: Applied Science, 1975.
[26] Barton J, Capek I. In: Horwood E, editor. Radical polymerization in disperse systems. Chichester and Veda, Bratislava, 1994.
[27] Kast H, Funke W. Makromol Chem 1981;182:1553.
[28] Roe CP. Ind Engng Chem 1968;60:20.
[29] Fitch RM, Prenosil MB, Sprick KJ. J Polym Sci C 1969;27:95.
[30] Hansen FK, Ugelstad J. J Polym Sci Polym Chem Ed 1978;16:1953.
[31] Chern CS, Lin CH. Polymer 1998;40:139.
[32] Garti N, Aserin A. Adv Colloid Interface Sci 1996;65:37.
[33] van der Hoff BME. Adv Chem Ser 1962:34.
[34] Capek I, Chern CS. Adv Polym Sci (in press).
[35] Bibette J, Calderon FL, Poulin P. Rep Prog Phys 1999;62:969.
[36] Miller CM, Sudol ED, Silebi CA. Macromolecules 1995;28:2772.